A Rational Design Equation for Galloping Power Lines

M. L. Lu, and J. K. Chan

***Abstract*-- A dimensionless galloping amplitude is found to be fairly constant for a given ice model, regardless of power line parameters, through fairly extensive parametric studies by using an existing hybrid finite element (FE) and three-degree-of-freedom (3DOF) computer software. This finding leads to a simple and rational design equation for estimating galloping amplitude for both single and bundle conductors with either suspension or deadend supports. Field galloping data observed in North America is used to calibrate the proposed design equation. Fairly good agreement is reached between the two results. The proposed design equation is further examined in detail to reveal the effects on the galloping amplitude of a conductor's diameter, tension, span length, and end condition.**

The proposed equation provides an additional tool to transmission engineers in determining tower head configurations including those of UHV lines.

***Index Terms*-- Conductor; design; galloping; icing; overhead line; wind.**

I. Introduction

GALLOPING is a wind induced, low frequency, large amplitude vibration generally caused by un-symmetric icing on overhead power line conductors [1]. Its occurrence may result in severe damage to a power line either electrically or mechanically so that galloping is one of the important considerations in designing power lines in an ice prone region.

Galloping has been investigated quite extensively since 1930's [2]. As a result, different numerical models are available for analyzing galloping power lines [3-10]. In such an analysis, assumptions have to be made on the shape of ice and its orientation, its variation over a span (uniform or non-uniform), wind pattern, damping properties of a line, etc. so that an arbitrary magnitude of galloping may be achieved by simply manipulating on the assumed parameters. Thus, the absolute magnitude of galloping as found from a numerical model may not be very reliable. This is why a numerical galloping model is hardly used directly in power line design practice. Instead, some empirical equations are often used to estimate design galloping magnitude [11-15]. Different methods could lead to not only quite different galloping magnitudes, but also different trends. Some of the methods assumed that the one-loop galloping amplitude is a constant factor of corresponding conductor sag, regardless of span length and conductor diameter [11, 13, 14]. Some considered the ratio of the galloping amplitude to the corresponding sag to be dependent on span length [12]. One method even considered conductor diameter dependency [15]. Most of the methods considered only one-loop galloping. A few also considered two-loop galloping [13]. Some methods distinguished a suspension end from a deadend [12], and some did not [11, 15]. All these methods were established empirically based on field galloping data. While field data are very useful, they often contain large uncertainty so that the resulting trends might not always be true.

Proper non-dimensionalization is the key to a simple design equation so that the number of contributing factors can be minimized. Most of the above mentioned empirical equations used the ratio of galloping amplitude to the corresponding sag [11-14], or the galloping amplitude to the conductor diameter [15]. A good discussion on different options of non-dimensionalization for galloping amplitude was given in [1].

In this paper, a previously developed, hybrid finite element (FE) and three-degree-of-freedom (3DOF) galloping software is used as the tool for parametric study. It is believed that a properly developed numerical model would be able to predict a correct trend. Based on these trends, a rational design equation may be established by further calibrating against field galloping data for the absolute values.

II. Parametric Study

A hybrid FE-3DOF galloping software was developed previously [8, 9] using a FE model to compute mode shapes [7] and a 3DOF model to perform galloping analysis [5, 6]. The software can accommodate both single and bundle conductors. Both suspension and deadend conditions are allowed. In addition, detuning pendulums [14] or hybrid nutation dampers [9, 16, 17] may be added as galloping control measures. This software is used as a parametric study tool.

In the following parametric study, data in Table I are used as inputs. In the table, the equivalent density of a conductor is defined so that it is related to the mass of the conductor per unit length, m_C, by

M. L. Lu is with BC Hydro, 6911 Southpoint Drive, Burnaby, BC, V3N 4X8, Canada (e-mail: mingliang.lu@bchydro.com).

J. K. Chan is with Electric Power Research Institute, Palo Alto, CA 80523 USA (e-mail: jchan@epri.com).

$$m_C = \rho_C \pi D_C^2 / 4 . \quad (1)$$

It is found that ρ_C is fairly constant for ACSR conductors. The value of 2550 kg/m^3 is approximately the average for all ACSR conductors.

TABLE I
SUMMARY OF THE BASIC INPUT DATA USED IN THE PARAMETRIC STUDY

Parameter	Symbol	Dimension	Range	Default
Diameter of a subconductor	D_C	mm	10-40	30
Span length	L	m	50-500	300
Equivalent density of conductor	ρ_C	kg/m^3	2550	2550
Catenary constant of conductor	C	m	500-3000	2000
Elastic modulus of conductor	E	MPa	65000	65000
Number of subconductors	N_C	N/A	1-4	1, 2
Spacing of subconductors	S_C	m	0.45	0.45
A conductor's plunge damping ratio	ζ_y	--	0.001	0.001
A conductor's swingback damping ratio	ζ_z	--	0.001	0.001
A conductor's twist damping ratio	ζ_t	--	0.003	0.003
Side wind speed	V_W	m/s	5-20	10

In addition, a conductor's catenary constant is defined by

$$C = T / (m_C g) . \quad (2)$$

The parameters in Table I provide fairly wide ranges to cover most of the power line situations.

Ice deposit is probably the most important factor for the occurrence of galloping. An ice accreted on a conductor can take different shapes and orientations [1, 9, 18]. It is impossible to encompass all the variations in the present parametric study. Therefore, three most representative ice shapes are considered here. They are: a thin crescent ice (C2), a thick crescent ice (C7), and a D-shaped ice (C11), as illustrated in Fig. 1. These shapes are most susceptible to galloping. They were obtained from outdoor freezing rain simulations [3, 19], and are good approximation to those observed on actual power lines. Their aerodynamic properties were measured in a wind tunnel [3, 19] and were given in Table II.

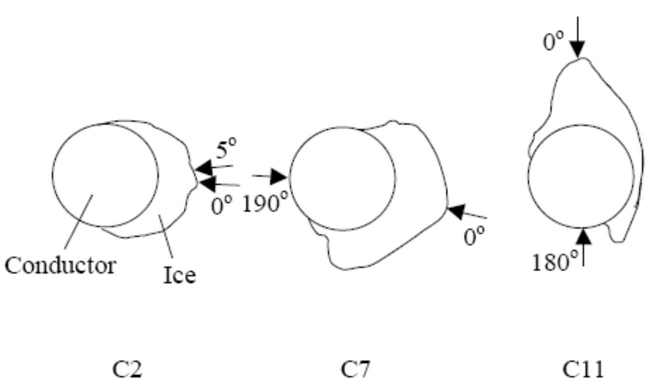

Fig. 1. The three ice shapes and their static orientations considered in the parametric study.

It is assumed in this study that ice is distributed uniformly over the span and, for a bundle conductor, the ice shape is assumed to be identical on all the subconductors. These assumptions may not strictly true. Ice tends to be less eccentric towards the midspan as a result of the conductor's greater torsional flexibility [9]. In addition, about 20% more ice mass has been observed, in a freezing rain experiment, on the windward compared with the leeward subconductor of a twin bundle presumably as a result of the airflow interference between the two subconductors [19]. The impact of these variations could be the subject of future studies.

Moreover, only one-loop and two-loop galloping events are considered as they are the ones observed most frequently in the field and are currently assumed in the design of transmission lines.

TABLE II
SUMMARY OF THE ICE RELATED COMPUTER INPUT

Ice model $^+$	C2-5	C7-190	C11-180
θ_{static} (deg)	5	190	180
a_{y0} $^{++}$	− 0.22290	0.67459	1.35755
a_{y1}	− 0.49329	− 0.53592	− 2.08210
a_{y2}	0.67073	− 4.34461	− 0.02880
a_{y3}	8.07320	9.47529	5.07790
a_{z0}	0.87938	1.28782	0.87200
a_{z1}	0.09344	− 0.19867	− 0.66440
a_{z2}	0.22738	− 0.56696	0.21960
a_{z3}	0.36018	1.06665	0.30950
$a_{\theta 0}$	− 0.01691	0.27763	0.16030
$a_{\theta 1}$	− 0.04997	0.17882	0.18740
$a_{\theta 2}$	0.48209	−1.01714	0.69240
$a_{\theta 3}$	3.16518	1.14757	0.03230

Note: + An ice model is designated by the symbol for an ice shape followed by the static orientation to a side wind, θ_{static}.
++ a_{yi}, a_{zi}, $a_{\theta i}$ are the aerodynamic coefficients in plunge, swingback and twist, respectively.

A. Non-dimensionalizaiton of galloping amplitude

To reduce the number of variables, galloping amplitude is non-diemensionalized. Different options were evaluated against numerical experiments. It is found that the following dimensionless galloping amplitude gives the least variation

$$\eta = Af / V_W \quad (3)$$

where A is the galloping amplitude in plunge, V_W is the side wind speed (normal to the conductor), and f is the natural frequency in the plunge (vertical) direction during galloping. As will be shown in the detailed parametric study that follows, the η value appears to be fairly constant for a given ice shape and its orientation, regardless of conductor diameter, conductor tension, conductor configuration, span length, end condition, and wind condition. In contrast, the galloping amplitude may be non-dimensionalized by either the sag or the conductor diameter, but the resulting values are highly variable.

Notice that Eq. (3) is consistent with the Hunt-Richards method [20]. The same dimensionless galloping amplitude was considered as one of the options in [1] in analyzing field data. The approach has not yet been widely accepted, presumably due to lack of justification.

B. Effect of a conductor' configuration on η

A phase conductor may contain one or more subconductors. To examine the bundle effect, five configurations are compared. They are: a single conductor (S), a twin bundle with a horizontal (2H) or a vertical (2V) arrangement, a triple bundle with a Δ-like (3A) or a ∇-like (3V) configuration, and a quad-bundle with a square configuration (Q). For each configuration, three ice models (C2-5, C7-190, and C11-180) and three catenary constant C values (1000m, 2000m, and 3000m) are considered. Otherwise, the default values given in Table I are adopted. In particular, D_C = 30mm, L = 300m. The computed η values for all the combinations involved are summarized in Fig. 2. There, for a given conductor configuration and a given ice model, there are three data points, which correspond to C = 1000m, 2000m and 3000m, respectively, from left to right.

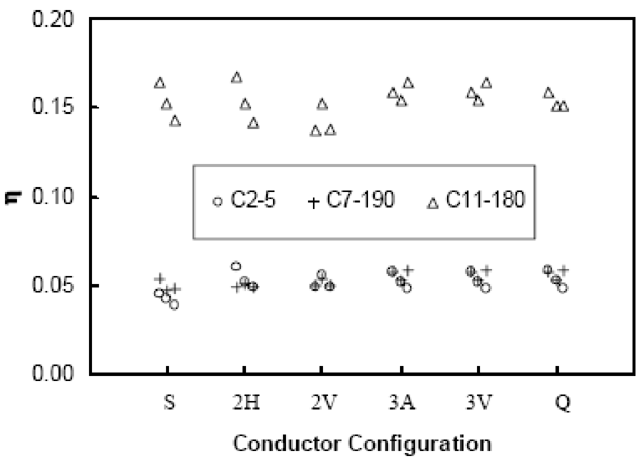

Fig. 2. Computed results showing the effect of a conductor's configuration on the η value.

Fig. 2 shows that the η value is fairly constant for a given ice model, regardless of different conductor configurations. Fig. 2 also indicates that C2-5 and C7-190 produces comparable galloping amplitude, while C11-180 produces approximately triple the galloping amplitude of the other two ice models.

As a conductor's configuration does not appear to affect the η value significantly, only a single conductor (S) and a twin bundle with a horizontal arrangement (2H) are considered in the further analyses that follow.

C. Effect of a conductor's end condition on η

The end of a conductor span may be suspended or deadended. To evaluate the effect, the same three ice models are used. In addition, the catenary constant C, span length L, and conductor diameter D_C are varied one at a time with default values for other parameters. The η values are computed for otherwise the same spans but one with suspension-suspension (S-S) supports and the other with deadend-deadend (D-D) supports. The results are summarized in Fig. 3 for both single (S) and twin bundle conductors (2H), where the solid and hollow data points correspond to a D-D support (noted by D as in C2-D) and a S-S support (noted by S as in C2-S), respectively. It can be seen from Fig. 3 that the end support condition has negligible effect on the resulting η value. Thus, only the D-D support will be considered hereafter. Again, Fig. 3 shows that the η value is fairly constant for a given ice model.

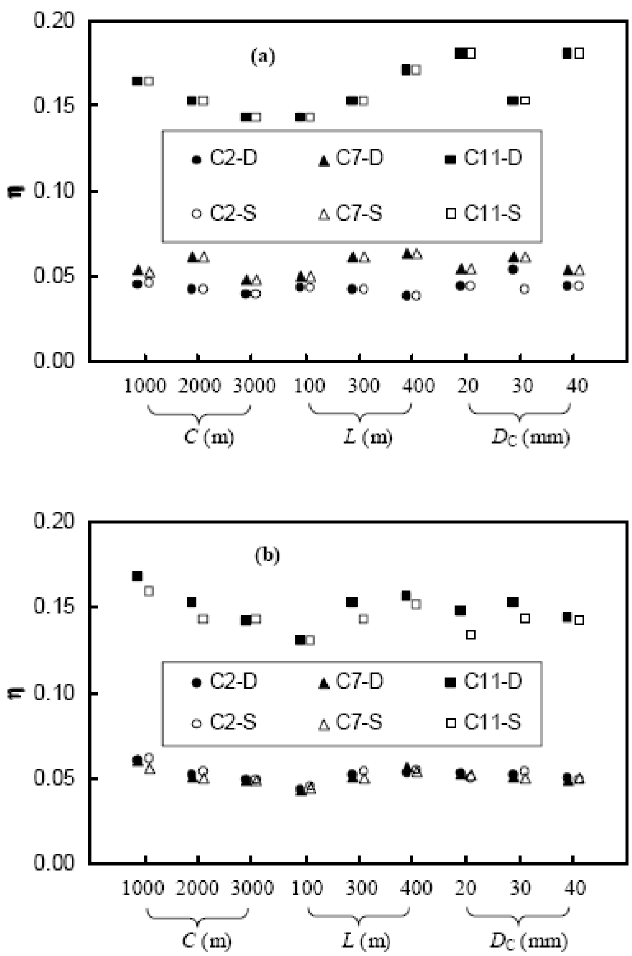

Fig. 3. Computed results showing the effect of a conductor's end support on the η value for (a) single conductors, S; and (b) twin bundle conductors, 2H.

D. Effect of conductor diameter on η

To examine the effect of the conductor diameter on the

η value, the three ice models and two conductor configurations (S and 2H) are used. For a given ice model and a given conductor configuration, the η values are determined for the conductor diameter of 10mm, 20mm, 30mm and 40mm, with the remaining parameters taking the default values. The results are summarized in Fig. 4, which shows that the conductor diameter appears to have minor effect on the η value.

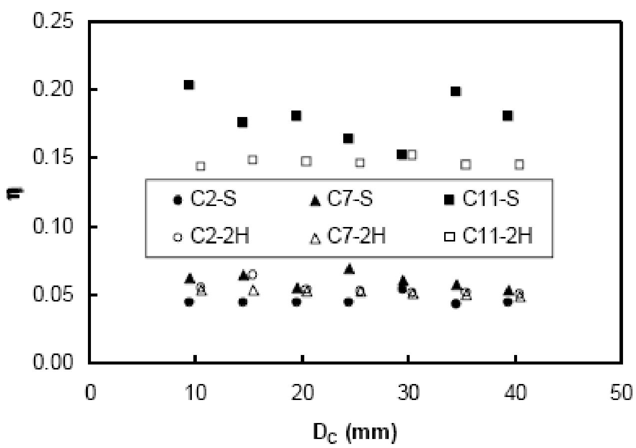

Fig. 4. Computed results showing the effect of a conductor's diameter, D_C, on the η value for both single conductors, S, and twin bundle conductors, 2H, under the three icing conditions (C2-5, C7-190, and C11-180).

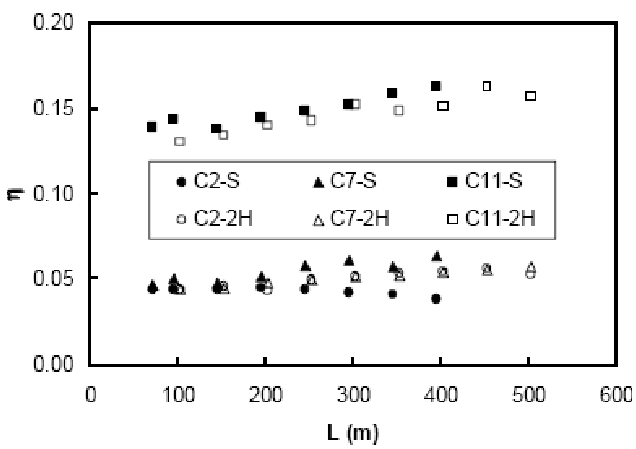

Fig. 5. Computed results showing the effect of a conductor's span length, L, on the η value for both single conductors, S, and twin bundle conductors, 2H, under the three icing conditions (C2-5, C7-190, and C11-180).

E. Effect of span length on η

To examine the effect of the conductor span length on the η value, the three ice models and two conductor configurations (S and 2H) are used again. For a given ice model and a given conductor configuration, the η values are computed for a span length of 50m to 400m for single conductors, and 100m to 500m for twin bundle conductors, respectively, with the remaining parameters taking the default values. The results are plotted in Fig. 5, which indicates that the span length appears to have minor effect on the η value, too.

F. Effect of a conductor's static tension on η

A conductor's static tension may be expressed more conveniently in terms of the catenary constant, *C*. To examine the effect of a conductor's catenary constant *C* on the η value, the three ice models and two conductor configurations (S and 2H) are used once more. For a given ice model and a given conductor configuration, the η values are determined for the *C* values of 500m to 3000m for both single conductors (S) and twin bundle conductors (2H), with the remaining parameters taking the default values. The results are plotted in Fig. 6, which indicates that the *C* value appears to have minor effect on the η value, too.

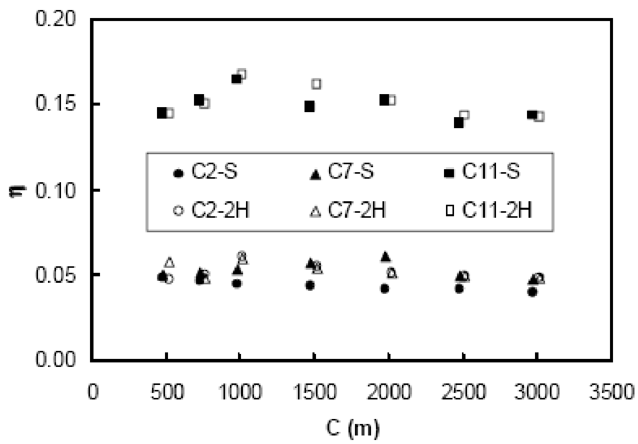

Fig. 6. Computed results showing the effect of a conductor's catenary costant, *C*, on the η value for both single conductors, S, and twin bundle conductors, 2H, under the three icing conditions (C2-5, C7-190, and C11-180).

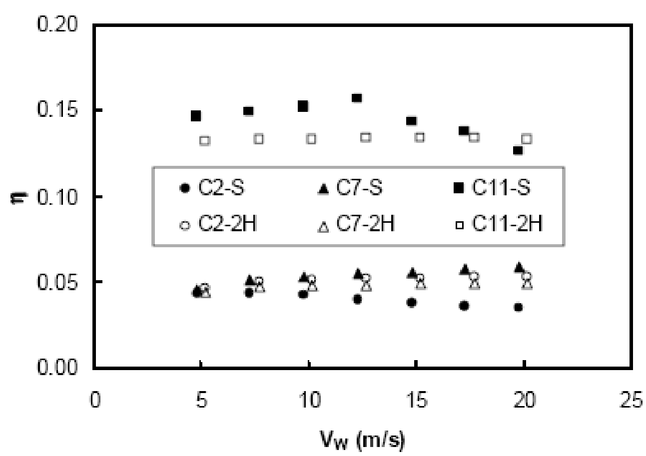

Fig. 7. Computed results showing the effect of a side wind's speed, V_W, on the η value for both single conductors, S, and twin bundle conductors, 2H, under the three icing conditions (C2-5, C7-190, and C11-180).

G. Effect of a side wind's speed on η

Similarly a side wind's speed, V_W, on the η value is examined in Fig. 7, which indicates that the effect appears to be minor, too.

H. Concluding remarks

It may be concluded from the above detailed parametric study that the non-dimensionalized galloping amplitude, η, appears to be fairly constant for a given ice model, regardless of possible changes in line parameters. Such a conclusion also confirms that the parameter is properly selected. As η is almost solely dependent on the ice model (its shape and orientation), the parameter may be used conveniently to measure the severity of galloping for a given geographical zone.

III. Design Equation

A. Basic equation

Practically, the η value may be viewed as a constant for a given ice model, regardless of line parameters. Thus, the galloping amplitude in plunge, A, may be determined by the following equation

$$A = \eta V_W / f \tag{4}$$

where f is a conductor's natural frequency in plunge during galloping. V_W is the side wind speed perpendicular to the conductor. It is evident that f represents the power line's effect on galloping, while η and V_W represent, collectively, the meteorological effect.

In Eq. (4), f can be calculated fairly easily with accuracy, as will be discussed in the next subsection. Both η and V_W should be determined statistically from field galloping observations due to the large uncertainties associated with icing conditions. It is difficult and unnecessary to distinguish between the values of η and V_W. Instead, it is practically more convenient to combine the two parameters into a single one. Thus, Eq. (4) may be written as

$$A = G / f \tag{5}$$

where G may be called the galloping factor, and is defined by

$$G = \eta V_W . \tag{6}$$

Notice that G has the same dimension as the wind speed.

B. Determining the plunge frequency f

The natural frequencies of a sagged conductor span in plunge with both ends fixed (i.e. D-D) is given by the following equation

$$f = \frac{k}{L}\sqrt{\frac{T}{m}} \tag{7}$$

where L is the span length, T is the static conductor tension, and m is the (iced) conductor mass per unit length. k = 1 for two-loop galloping. For one-loop galloping, k should be solved from the following equation [21]

$$\tan(k\pi) = k\pi - \frac{4(k\pi)^3}{\lambda^2} \tag{8}$$

where λ is defined as

$$\lambda = \frac{mgL}{T}\sqrt{K_C \frac{L}{T}} . \tag{9}$$

Here K_C is the conductor stiffness, or

$$K_C = EA / L \tag{10}$$

in which E is the equivalent elastic modulus of the conductor; and A is the cross sectional area of the conductor.

Eq. (8) may be conveniently approximated by the following equation

$$k = 0.5 + 0.93[1 - \exp(-0.02\lambda^2)] . \tag{11}$$

The k values from Eq. (11) and Eq. (8) are compared in Fig. 8. Good agreement between the two results can be observed.

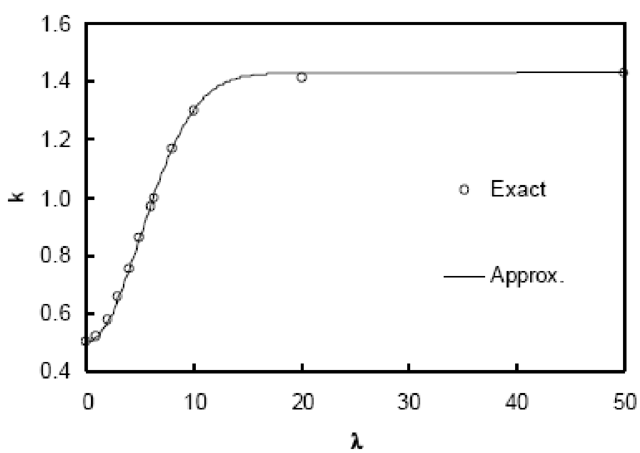

Fig. 8. Comparing k values from the exact solution of Eq. (8) to the approximate solution of Eq. (11).

For a conductor span with an end support of either S-S or D-S (i.e. deadend-suspension), the same equations can be used, except K_C in Eq. (9) should be modified to include the effects of the neighboring spans and the suspension insulators. That is, instead of using Eq. (10), the following equation should be used to determine K_C

$$1/K_C = 1/(EA/L) + 1/K_{S,L} + 1/K_{S,R} \tag{12}$$

where $K_{S,L}$ and $K_{S,R}$ are the stiffness of the left and right end supports, respectively. $K_{S,L}$, for example, is given by [3, 5]

$$K_{S,L} = K_{ST,L} + K_{I,L} \tag{13}$$

where, $K_{ST,L}$ and $K_{I,L}$ are the stiffness of the left conductor span and left suspension insulator string, respectively. They are given, respectively, by

$$1/K_{ST,L} = 1/(EA/L_L) + (mgL_L/T)^3/(12mg) \qquad (14)$$

and

$$K_{I,L} = [m(L+L_L) + M_I]g/(2L_I) \qquad (15)$$

where L_I and M_I are the length and mass of the suspension insulator string, respectively. is the length of the left span.

If a conductor span's left end, say, is a deadend, then $K_{S,L} = \infty$. Thus, Eq. (12) will reduce to Eq. (10) if both ends are deadended (i.e. D-D).

The finite element based computer model [7] is used to validate the above simple analytical approach to the natural frequency of a sagged conductor span. For this purpose, it is assumed that

$E = 6.5 \times 10^{10}$ Pa; $D_C = 30$ mm;

$m = 1.8025$ kg/m; $M_I = 51$ kg;

and $L_I = 1.5$ m.

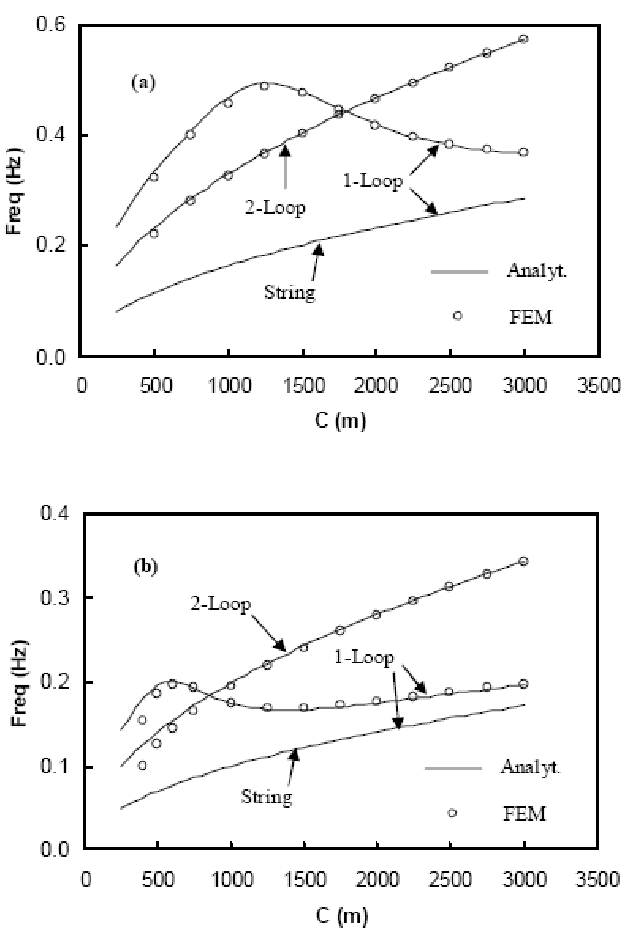

Fig. 9. Comparing the plunge frequencies of first two loops from the simple analytical equations to those from the finite element based computer model [7] for (a) a D-D span; and (b) a S-S span.

In addition, two end conditions are considered: D-D and S-S. For the D-D situation, $L = 300$ m; and for the S-S situation, $L = L_L = L_R = 500$ m. Use of the longer span for a S-S situation is to enhance the sag effect on the plunge frequency.

Fig. 9 compares the results of the first two natural frequencies (one-loop and two-loop) in plunge from the above simple method (as noted by "Analyt." and those from the finite element model (as noted by "FEM") for various catenary constant C values. A good agreement can be observed between the two results.

Notice that a one-loop frequency is higher than the corresponding two-loop frequency for the D-D span at $C <$ 1800m, and for the S-S span at $C <$ 900m. Thus, a two-loop galloping will prevail under such a situation. One-loop galloping will prevail otherwise.

In addition, according to the tensioned string theory (without sag), k = 0.5 for the one-loop, plunge frequency. The resulting one-loop plunge frequency (denoted by "String") is compared with the frequency for a sagged conductor, also given in Fig. 9. It can be observed from Fig. 9 that the existence of sag tends to increase the one-loop, plunge frequency quite significantly. The two results tend to converge with high tension (i.e. high C value) as one may expect, because higher tension leads to lower sag.

C. Determining the galloping factor G

G may be computed numerically if the ice shape and its static orientation as well as the side wind speed are all known. However, in reality, the icing conditions are often unknown or unclear. This is particularly true for designing a new power line. In addition, some line parameters, such as damping ratios in individual directions, are highly uncertain. Thus, the absolute G values as obtained from a numerical study might not be realistic. Therefore, the design G value should be derived from field galloping observations, and it should lead to an upper bound estimate of galloping amplitude when compared with the field galloping data.

Currently there are two sets of field galloping data that are available in the literature [1, 14]. They are now used to determine the design G value. As the field data were collected in North America, the resulting design G value should be viewed as being applicable to North America only.

The two data sets, one from EPRI [1] and one from Ontario Hydro [14], are plotted in Figs. 10 and 11, respectively, in terms of the double galloping amplitude, Y, non-dimensionalized by the corresponding sag, S, versus the span length, L. Also given in the figures are the predictions from the present simple method [as represented by Eq. (5)] by assuming that G = 0.75m/s, C = 2000 m, and D_C = 25.4mm. The assumed C and D_C values are believed to be representative of their actual values on average. Notice that the double galloping amplitude Y is related to the corresponding single amplitude A by $Y = 2A$.

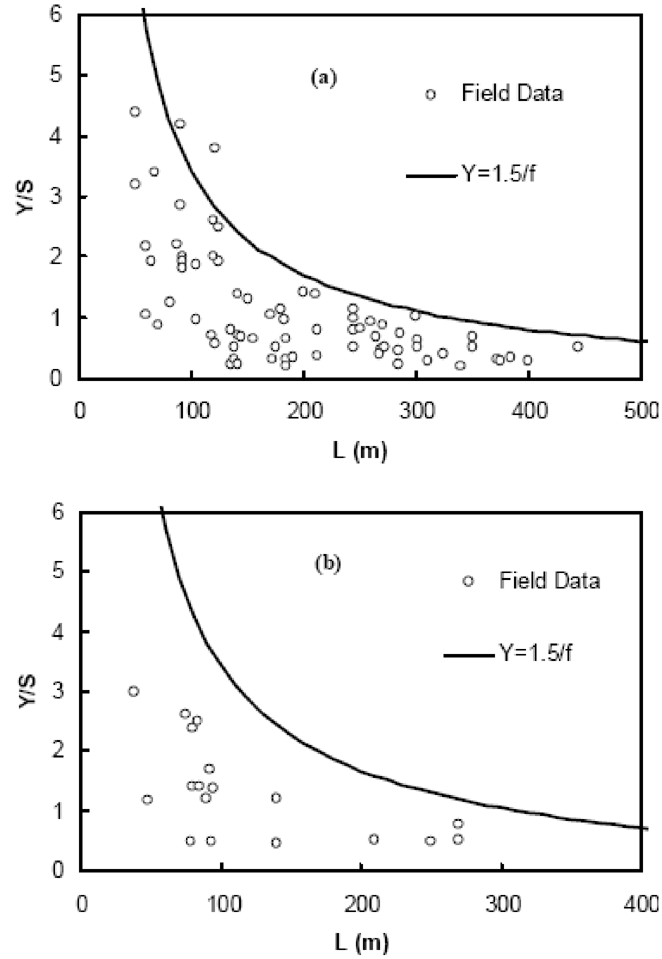

Fig. 10. Comparing EPRI field galloping data [1] to the predictions from Eq. (5) with G = 0.75m/s for (a) suspension spans; and (b) deadend spans.

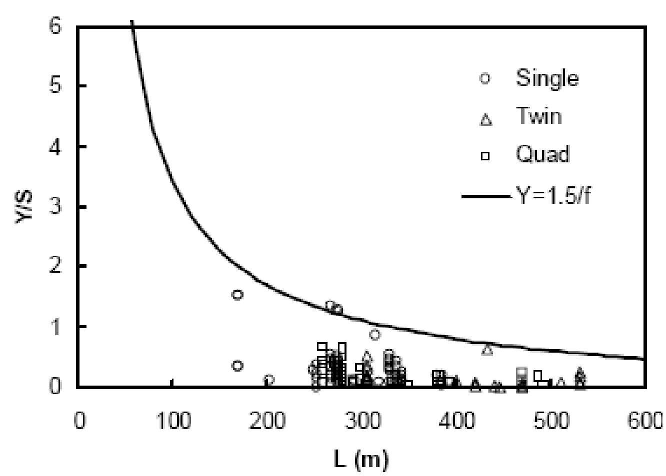

Fig. 11. Comparing Ontario Hydro field galloping data [14] to the predictions from Eq. (5) with G = 0.75m/s for various conductor configurations.

It can be seen from Figs. 10 and 11 that, with G = 0.75m/s, Eq. (5) appears to predict an upper bound, galloping amplitude fairly nicely for most of the field data. Thus, 0.75m/s may be used as the design G value in North America, if local galloping experience is lacking. Therefore, the design equation (5) becomes

$$A = 0.75 / f \tag{16}$$

or

$$Y = 1.50 / f \tag{17}$$

where f is in Hz; both A and Y are in m.

IV. Discussion

Eq. (17) is examined in detail next in attempt to reveal any trends it may contain. For this study, the following default values are assumed if they are not noted otherwise: $E = 6.5 \times 10^{10}$ Pa; C = 2000 m; D_C = 25.4 mm; $\rho_C = 2550$ kg/m3; L_I = 1.5 m; M_I = 51 kg; and the equivalent radial ice thickness b = 6.35 mm [18].

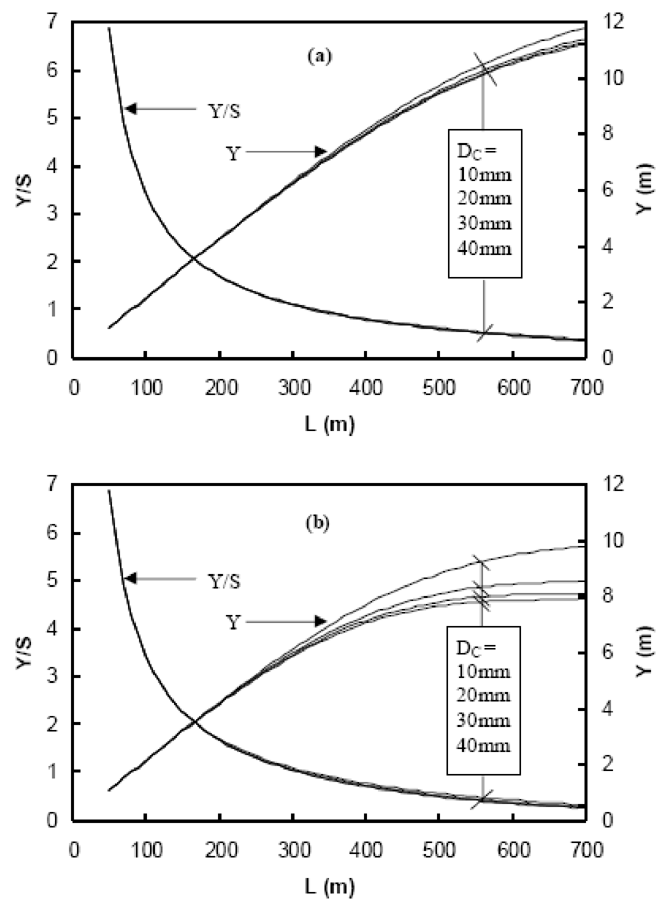

Fig. 12. Summarized results showing the effect of conductor diameter, DC, on Y or Y/S for (a) S-S spans; and (b) D-D spans.

A. Effect of conductor diameter

Fig. 12 summarizes the results from Eq. (17) showing the effect of conductor diameter, D_C, on both Y/S and Y for various span lengths. It can be seen that D_C hardly affects Y/S particularly for relatively short spans. However, D_C appears to affect Y to some extent for relatively long spans. Y tends to decrease a little bit with greater conductor diameter. Moreover, D_C tends to have a greater effect on Y for a D-D span than for an otherwise the same S-S span.

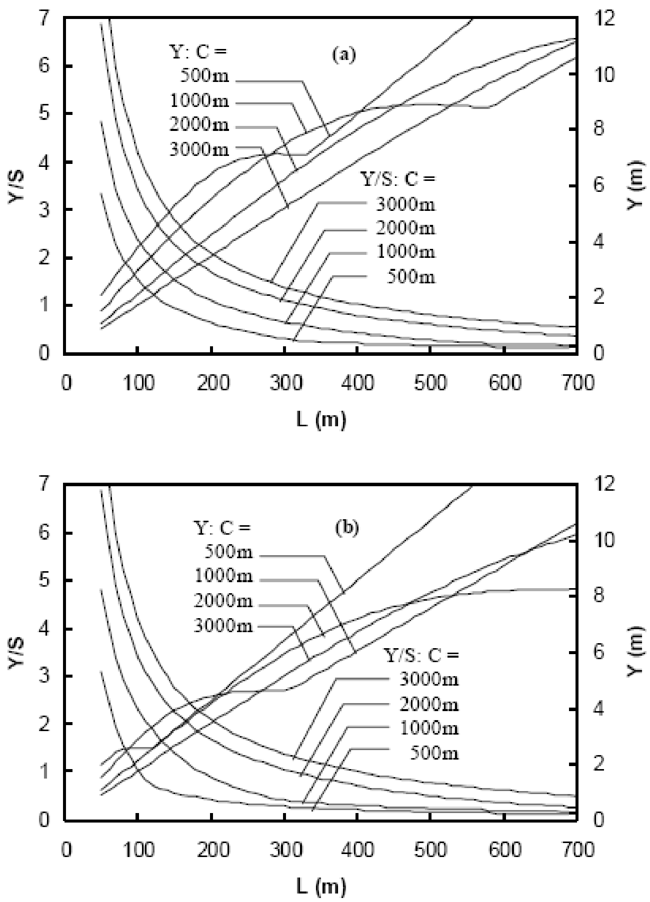

Fig. 13. Summarized results showing the effect of the catenary constant, C, on Y or Y/S for (a) S-S spans; and (b) D-D spans.

B. Effect of tension

Fig. 13 gives the results from Eq. (17) showing the effect of conductor tension (as represented by the catenary constant, C) on both Y/S and Y for various span lengths. Clearly, the conductor tension (or alternatively, the catenary constant, C) has a significant effect on both Y/S and Y, regardless of span length or end conditions.

It is interesting to observe that Y/S tends to increase, invariably, with greater tension. However, the trend becomes complicated for Y because of the sag effect. For S-S spans (Fig. 13a), over the normal range of C between 1000m and 3000m, increasing tension tends to decrease galloping amplitude, Y, for spans up to approximately 450m, because the associated sag effect is not significant enough. The same is true for D-D spans but only for spans less than approximately 200m, as shown in Fig. 13b. Such an upper bound span limit tends to be longer for higher conductor tension. For spans beyond this limit the sag will modify the one-loop, plunge frequency significantly so that at a certain point the one-loop frequency may catch up the corresponding two-loop frequency. Then two-loop galloping will prevail over one-loop galloping. This transition process may cause the reversed trend that a tension increase results in higher galloping amplitude. A transition from a one-loop galloping to a two-loop galloping is clearly shown in Fig. 13 by those knee points on the curves. As one may expect, the knee point occurs at a shorter span for a lower tension or a stiffer end support.

C. Effect of span length

It can be observed from Figs. 12 and 13 that Y/S tends to decrease with longer span consistently. In addition, such a decrease becomes less sensible for longer spans.

As for the galloping amplitude, Y, it tends to increase with longer span as one may expect. Moreover, it is interesting to notice that the variation of the galloping amplitude Y with the span length L may be distinguished advantageously into two stages that are divided by the knee point. Before the knee point, one-loop galloping will prevail. Two-loop galloping will prevail otherwise. The galloping amplitude, Y, tends to grow slower for a longer span until the knee point is met. After the knee point is exceeded, the galloping amplitude tends to grow much faster than before at almost a constant rate.

D. Effect of a span's end condition

Comparison of Figs. 12a and 12b appears to indicate that a D-D span gallops less than a S-S span for the same conditions otherwise. However, this may not be always true as may be found by comparing Figs. 13a and 13b that a reversed trend may occur at low tension of, say C = 500m.

In addition, it can be seen by comparing Figs. 13a and 13b that the knee point occurs at a shorter span for a D-D span than for a S-S span with the same conditions otherwise. This implies that a two-loop galloping may occur more likely on D-D spans than S-S spans.

V. Conclusion

The following conclusions may be made from this study.

(1) A dimensionless parameter for galloping amplitude has been found whose value is fairly constant for a given ice model regardless of different line conditions. A fairly extensive parametric study were undertaken using an existing hybrid FE-3DOF galloping analysis software to support this finding.

(2) A rational and simple design equation for galloping amplitude has been established based on the above finding. The equation contains the natural frequency

in plunge for a sagged conductor span. An approximate, analytical solution has been proposed for the frequency with proper corrections for the sag effect and the end conditions. The predicted frequency agrees reasonably well with that from a finite element transmission line model.

(3) The galloping factor *G* can be used to measure the severity of galloping. With the galloping factor *G* of 0.75 m/s, the proposed design equation is able to envelop the available field galloping data in North America closely. This number may be used in North America for power line design if local galloping experience is lacking.

(4) The effects of a conductor's diameter, tension, span length and end condition on the design galloping amplitude have been evaluated using the proposed design equation. These effects may provide useful guidance to power line design engineers in terms of galloping trends.

VI. References

[1] EPRI, *Transmission Line Reference Book: Wind-Induced Conductor Motion*, Electric Power Research Institute, Palo Alto, CA, 1979.

[2] J. P. Den Hartog, "Transmission line vibration due to sleet," *AIEE Trans*. Vol. 51, pp. 1074-1076, 1932.

[3] Manitoba Hydro, "Modeling of conductor galloping," Vol. I and II, CEA Report, Project No. 321 T 672, Canadian Electrical Association, 1992.

[4] Manitoba Hydro, "Modeling of single conductor galloping: Phase II," CEA Report, Project No. 321 T 672A, Canadian Electrical Association, 1995.

[5] P. Yu, Y. Desai, A. H. Shah, and N. Popplewell, "Three-degree-of-freedom model for galloping, Part I: formulation," *J. Engrg. Mech., ASCE*, vol. 119, no. 12, pp. 2404-2425, 1993.

[6] P. Yu, Y. Desai, N. Popplewell, and A. H. Shah, "Three-degree-of-freedom model for galloping, Part II: solutions," *J. Engrg. Mech., ASCE*, vol. 119, no. 12, pp. 2426-2448, 1993.

[7] Y. Desai, P. Yu, A. H. Shah, and N. Popplewell, "Finite element modeling of transmission line galloping," *Comput. Struct*., vol. 57, pp. 469-489, 1995.

[8] Q. Zhang, N. Popplewell, and A. H. Shah, "Galloping of bundle conductor," *J. Sound Vibr.*, vol. 234, no. 1, pp. 115-134, 2000.

[9] M. L. Lu, "Predicting ice accretion and alleviating galloping on overhead power lines," PhD Thesis, Department of Civil Engineering, University of Manitoba, Winnipeg, Manitoba, Canada, 2001.

[10] J. Wang, and J. L. Lilien, "Overhead electrical transmission line galloping: a full multi-span 3dof model, some applications and design recommendations," *IEEE Trans Power Delivery*, vol. 13, no. 3, pp. 909-916, 1998.

[11] A. E. Davison, "Ice-coated electrical conductors," Bulletin, Hydro-Electric Power Commission of Ontario, vol. 26, no. 9, pp. 271-280, 1939.

[12] P. F. Winkelman, "Investigations of ice and wind loads, galloping, vibrations and subconductor oscillations (Transmission line conductor problems)," U. S. Department of the Interior, Bonneville Power Administration, 1974.

[13] REA, "Design manual for high voltage transmission line," Bulletin 1724E-200, Rural Electrification Administration, United States Department of Agriculture, 1992.

[14] D. G. Havard, and C. J. Pon, "Use of detuning pendulums for control of galloping of single conductor and two- and four-conductor bundle transmission lines," 5th *IWAIS*, Tokyo, Japan. 1990

[15] J. L. Lilien, and D. G. Havard, "Galloping database on single and bundle conductors prediction of maximum amplitudes," *IEEE Trans. Power Delivery*, vol. 15, no. 2, pp. 670-674, 2000.

[16] M. L. Lu, N. Popplewell, A. H. Shah, and J. K. Chan, "Hybrid nutation damper for controlling galloping power lines," *IEEE Trans. Power Delivery*, vol. 22, no. 1, 2007.

[17] M. L. Lu, N. Popplewell, A. H. Shah, and J. K. Chan, "Nutation damper undergoing a coupled motion," *J. Vibration and Control*, vol. 10, no. 9, pp. 1313-1334, 2004.

[18] M. L. Lu, N. Popplewell, and A. H. Shah, "Freezing rain simulations for fixed, unheated conductor samples," *J. Applied Meteorology*, vol. 39, pp. 2385-2396, 2000.

[19] P. Stumpf, "Determination of aerodynamic forces for iced single and twin-bundled conductors," M. Sc. Thesis, Department of Mechanical and Industrial Engineering, University of Manitoba, Winnipeg, Manitoba, Canada, 1994.

[20] J. C. R. Hunt, and D. J. W. Richards, "Overhead line oscillations and the effect of aerodynamic dampers," *Proceedings IEE*, vol. 116, no. 11, pp. 1869-1874, 1969.

[21] H. M. Irvine, and T. K. Caughey, "The linear theory of free vibrations of a suspended cable," *Proc. R. Soc. Lon.* A. vol. 341, pp. 299-315, 1974.

VII. Biographies

M. L. Lu received his B.Eng. and M. Eng. degrees from Tongji University at Shanghai, China, in 1984 and 1987, respectively, and his Ph.D. degree from University of Manitoba at Winnipeg, Canada, in 2001, all in Civil Engineering. He has about 20 years' experience in transmission line analysis and design as a result of working for a Chinese laboratory, two Canadian utility companies, and as Consultant.

Dr. Lu has a wide scope of interests and expertise related to overhead power lines, which include: Aeolian vibration, galloping, and subspan oscillation; ice and wind loading; reliability based design; soils and foundations.

Dr. Lu is currently Senior Engineer, Overhead Transmission, BC Hydro, and is a Professional Engineer registered in the province of British Columbia.

J. K. Chan received his B.Sc. degree in electrical engineering from the University of Manitoba in 1971 and a M.Sc. degree in mechanical engineering from the same university in 1975. He worked for Manitoba Hydro from 1973 to early 2003 and was the head of transmission line designs when he left Manitoba Hydro for the Electric Power Research Institute. Mr. Chan is currently a program manager in the Power Delivery and Utilization sector of Electric Power Research Institute of USA.